ENGINEERING JOURNAL

Article

Ethylene/1-Hexene Copolymerization over Different Phases Titania-Supported Zirconocene Catalysts

Mingkwan Wannaborworn, Thanai Sriphaisal, and Bunjerd Jongsomjit*

Center of Excellence on Catalysis and Catalytic Reaction Engineering, Department of Chemical Engineering, Faculty of Engineering, Chulalongkorn University, Bangkok 10330, Thailand
*E-mail: bunjerd.j@chula.ac.th (Corresponding author)

Abstract. Ethylene/1-hexene copolymerization was performed over titania-supported zirconocene/dMMAO catalysts. Effects of titania having different phases on the catalytic activity and polymer properties were investigated. It was found that anatase titania exhibited the highest catalytic activity, and afforded copolymer with high 1-hexene incorporation among other titanias. According to TGA result, the stronger interaction between dMMAO and titania for anatase phase led to the highest catalytic activity, because the stronger interaction between cocatalyst and support would prevent the leaching of cocatalyst. Additionally, based on EDX mapping, a good dispersion of dMMAO over support surface is another reason for an increase in the catalytic activity. SEM analysis indicated that no significant change in polymer morphology was found for all supported catalysts. The incorporation of 1-hexene determined by ^{13}C NMR suggested that titania which possessed high amount of $[Al]_{dMMAO}$ over support surface showed high ability to incorporate 1-hexene. The random copolymers were produced in all systems.

Keywords: Metallocene, copolymerization, titania, heterogeneous catalyst.

ENGINEERING JOURNAL Volume 19 Issue 5
Received 20 February 2015
Accepted 11 May 2015
Published 31 October 2015
Online at http://www.engj.org/
DOI:10.4186/ej.2015.19.5.55

DOI:10.4186/ej.2015.19.5.55

1. Introduction

Nowadays, polyethylene is one of the most widely used polymers in daily life, especially the linear low density polyethylene (LLDPE). Due to its light weight, high impact strength and excellent chemical resistance as well as being cost effective, therefore, LLDPE has been used in many applications such as plastics bottles, containers, pipes and house wares [1, 2]. LLDPE is commonly produced by the copolymerization of ethylene with α-olefins using Ziegler-Natta and metallocene catalysts.

Comparing two conventional catalysts, metallocenes are single site. They offer high catalytic activity and make LLDPE with narrow molecular-weight and chemical composition distribution, thus LLDPE produced from metallocene catalysts show considerably improved mechanical strength and physical properties compared to the conventional Ziegler-Natta [3–6]. However, the metallocene catalysts have some disadvantages such as lack of morphology control of polymer particle and reactor fouling when they used in homogeneous system [7, 8]. This leads to they are still not suitable to apply in an industrial-scale production. To overcome these drawbacks, many researchers have revealed that the supporting metallocene catalysts onto inorganic carriers is the most effective way. The supported metallocene catalysts require small amount of cocatalyst, resulted in cost reduction and they can control the polymer particle morphology as well as they can be applied for the gas- and slurry-phase polymerization processes. Therefore, the development of supported metallocene catalysts is very considered.

The inorganic carriers such as silica [9–11], alumina [12], magnesium chloride [13] and titania [14–16] are commonly employed for both ethylene homo- and copolymerization. The type of used support has an important influence on the polymer properties such as morphology, particle size and molecular weight. In this study, we chose titania as a support for the synthesis of LLDPE. In our previous works, we reported that the copolymerization of ethylene and 1-octene using titania supported *ansa*-dichlorodimthylfluorenyl titanium complex provided lower molecular weight copolymer with narrow molecular weight distribution compared to the use of silica and silica-titania supports [17]. According to the literature [18], the crystallite size of titania has a strong influence on the catalytic behavior for ethylene and 1-hexene copolymerization. We demonstrated that the catalytic activity increased with an increase of titania crystallite sizes. The larger size of nano-titania particle was used, the greater catalytic activity was obtained. Also, Domínguez A.M. et al. [19] prepared $(Fe(SO_4)_2(NH_4)_2)/TiO_2$ catalyst for ethylene polymerization and revealed that titania surface still remained a lot of hydroxyl group after calcination at high temperature, which have an effect on the metal complex anchoring. It is known that the hydroxyl group on the support surface plays a significant role in catalytic activity. The cocatalyt such as aluminoxane bonds to hydroxyl groups on the support surface, and then reacts with metallocene catalyst to generate active species for polymerization. Hence, the use of titania as catalyst support may be a promising way for better heterogeneous system.

In this work, we used titania with different phases as the support for metallocene catalyst to investigate the effect of phase composition on the catalytic activity and polymer properties for ethylene and 1-hexene copolymerization.

2. Experimental

2.1. Materials

All operations were performed under an argon atmosphere using a glove box and/or standard Schlenk techniques. Argon gas was purified by passing it through column packed with R3-11G copper catalyst, sodium hydroxide (NaOH) and phosphorus pentaoxide (P_2O_5), as ethylene gas (99.96% purity) was donated by the National Petrochemical Co., Ltd., Thailand. The *rac*-ethylenebis (indenyl) zirconium dichloride (*rac*-$Et[Ind]_2ZrCl_2$) as catalyst was supplied from Aldrich Chemical Company, Inc. Modified methylaluminoxane (MMAO) in toluene was donated by Tosoh , Akso, Japan. Trimethylaluminum (TMA, 2 M in toluene) was supplied by Nippon Aluminum Alkyls, Ltd., Japan. TiO_2 supports were purchased from Aldrich Chemical Company, Inc. Toluene was distilled over sodium/benzophenone before use. 1-hexene was purchased from Aldrich Chemical Company, Inc. which was dried over calcium hydride overnight and distilled under Argon gas prior to use.

2.2. Preparation of TiO_2

All TiO_2 supports were calcined under vacuum at 673 K for 6 h. prior to impregnation with dMMAO. The mixed phase TiO_2 support was mixed by physical method in the glove box after vacuum heating. 100% of anatase denoted as TiO_2 (A), where 100% of rutile denoted as TiO_2 (R). The mixed phase of anatase and rutile TiO_2 supports [50 wt% of TiO_2 (A) and 50 wt% of TiO_2 (R)] denoted as TiO_2 (M) was mixed by physical method.

2.3. Preparation of Dried-MMAO (dMMAO)

dMMAO was prepared according to the literature [20,21]. A toluene solution of MMAO was dried under vacuum for 6 h by evaporating solvent, TMA and Al(*i*Bu$_3$) (TIBA). The remaining TMA and TIBA were removed by washing with 100 mL of heptane for 7 times. The product was dried under vacuum to get white powder called dried-MMAO (dMMAO).

2.4. Preparation of dMMAO Impregnated on TiO_2 Supports (dMMAO/TiO_2)

An appropriate amount of dMMAO was added to the suspension of titania in 20 mL of toluene at room temperature. The mixture was stirred for 30 min, and then evaporated the solvent under vacuum. After the product was washed once with toluene and three times with hexane, it was further dried under vacuum for 6 h. The white powder of dMMAO impregnated on titania was obtained and denoted as dMMAO/TiO_2.

2.5. Polymerization

The copolymerization of ethylene and 1-hexene was carried out in a 100 ml semi-batch stainless steel autoclave reactor equipped with a magnetic stirrer. In the glove box, the desired amounts of zirconocene catalyst and TMA ($[Al]_{TMA}/[Zr]cat$ = 2500) were mixed together and stirred for 5 min for aging. Then, desired amounts of toluene and dMMAO/support were introduced into the reactor. The ratio of $[Al]_{dMMAO}/[Zr]_{cat}$ was fixed at 1135. After the mixture of zirconocene and TMA was injected into the reactor, the reactor was frozen in liquid nitrogen to stop reaction and 0.018 mol of 1-hexene was injected into the reactor. The reactor was evacuated to remove argon, and then it was heated up to polymerization temperature (343 K). Polymerization was started by feeding ethylene gas (total pressure 50 psi in the reactor) until the consumption of ethylene 0.018 mol (6 psi was observed from the pressure gauge) was reached. The reaction was terminated by adding acidic methanol. The obtained polymer was washed with methanol and dried at room temperature.

2.6. Characterization

2.6.1. Characterization of supports and catalyst precursor

N_2 physisorption: Measurement of BET surface area, average pore diameter and pore size distribution were determined by N_2 physisorption using a Micromeritics ASAP 2000 automated system.

X-ray diffraction: XRD was performed to determine the bulk crystalline phases of samples. It was conducted using a SIEMENS D-5000 X-ray diffractometer with CuK_α (l = 1.54439 Å). The spectra were scanned at a rate of 2.4^o min^{-1} in the range of 2 theta = 10-80^o.

Scanning electron microscopy and energy dispersive X-ray spectroscopy: SEM and EDX were used to determine the morphologies and elemental distribution throughout the sample granules, respectively. The SEM of JEOL mode JSM-6400 was applied. The EDX was performed using Link Isis series 300 program.

Thermo gravimetric analysis: TGA was performed using TA Instruments SDT Q 600 analyzer. The samples of 10-20 mg and a temperature ramping from 298 to 1273 K at 2 K/min were used in the operation. The carrier gas was N_2 UHP.

Inductively coupled plasma atomic emission spectrometer: ICP-AES by Perkin Elmer model PLASMA-1000 was employed to determine the content of aluminium ($[Al]_{dMMAO}$) of the catalyst precursor. The sample was dissolved by hydrofluoric acid (48%) 5 ml. The mixture was stirred and heated at 323 K over night. After the sample was completely dissolved, the solution was diluted to a volume of 100 ml prior to analysis.

X-ray photoelectron spectroscopy: The XPS analysis was performed using an AMICUS photoelectron spectrometer ESCA-3400 equiped with an Mg K_α X-ray as primary excitation and KRATOS VISION2 software. XPS elemental spectra were acquired with 0.1 eV energy step as a pass energy of 75 kV. The C 1s line was taken as an internal standard at 285.0 eV.

Transmission electron microscopy: TEM was used to determine the morphologies and crystallite size of TiO_2 supports. The sample was dispersed in ethanol before using TEM (JEOL JEM-2010) for micro structural characterization.

2.6.2. Characterization of polymer

The nuclear magnetic resonance: ^{13}C NMR spectroscopy was used to determine the triad distribution and 1-hexene incorporation indicating the copolymer microstructure. Chemical shifts were referenced internally to the $CDCl_3$ and calculated according to the literature [22]. Sample solution was prepared by dissolving 50 mg of copolymer in 1,2,4-trichlorobenzene and $CDCl_3$. ^{13}C NMR spectra were taken at 333 K using BRUKER AVANCE II 400 operating at 100 MHz with an acquisition time of 1.5 s and a delay time of 4 s.

Differential scanning calorimetry (DSC): Thermal analysis measurements were performed using a TA instrument 2910. The DSC measurements reported here were recorded during the second heating/cooling cycle with the rate of 10 K min^{-1}. This procedure ensured that the previous thermal history was erased and provided comparable conditions for all samples. Approximately 10 mg of sample was used for each DSC measurement.

Scanning electron microscopy and energy dispersive X-ray spectroscopy: SEM and EDX were performed to study the morphologies of polymer and elemental distribution within polymer matrix. The same equipment as mentioned before was employed.

3. Results and Discussion

3.1. Characteristics of Catalyst Support

In this study, we synthesized LLDPE by the copolymerization of ethylene and 1-hexene over zirconocene/dMMAO catalysts. Titania having different phases such as anatase, rutile and mixed phase were denoted as TiO_2 (A), TiO_2 (R) and TiO_2 (M), respectively and used as an inorganic support.

Table 1 summarizes the specific surface area, average pore diameter and pore volume for titania samples with different phases. The results show that the anatase titania possessed the highest surface area, pore diameter and pore volume, while the rutile phase showed the lowest textural properties among other ones. This observation is in good agreement with TEM analysis, which found that the smaller crystallite size of titania exhibited the higher surface area.

Table 1. Characteristics of different TiO_2 supports.

Types of support	Surface area (m^2g^{-1})	Average pore diameter (nm)	Pore volume ($cm^3\ g^{-1}$)	Crystallite size[a] (μm)
TiO_2 (A)	10.6	8.12	0.022	0.5-3
TiO_2 (M)	6.2	6.71	0.011	3-7
TiO_2 (R)	3.5	4.98	0.005	2-8

[a]Based on TEM measurement.

The XRD patterns of titania before and after impregnation with dMMAO are shown in Fig. 1. It can be seen that the strong diffraction peaks of anatase phase appears at 25° (major), 38°, 48°, 55°, and 63°, where the characteristic peaks of rutile are at 27° (major), 36°, 41°, and 54° [14, 18]. The mixed phase titania shows the presence of both anatase and rutile diffraction peaks. After impregnation with dMMAO, no new diffraction peak was observed for all systems. It was due to the highly dispersion of dMMAO over titania support and/or low amount of dMMAO impregnated on titania particle, thus the XRD patterns before and after impregnation were similar.

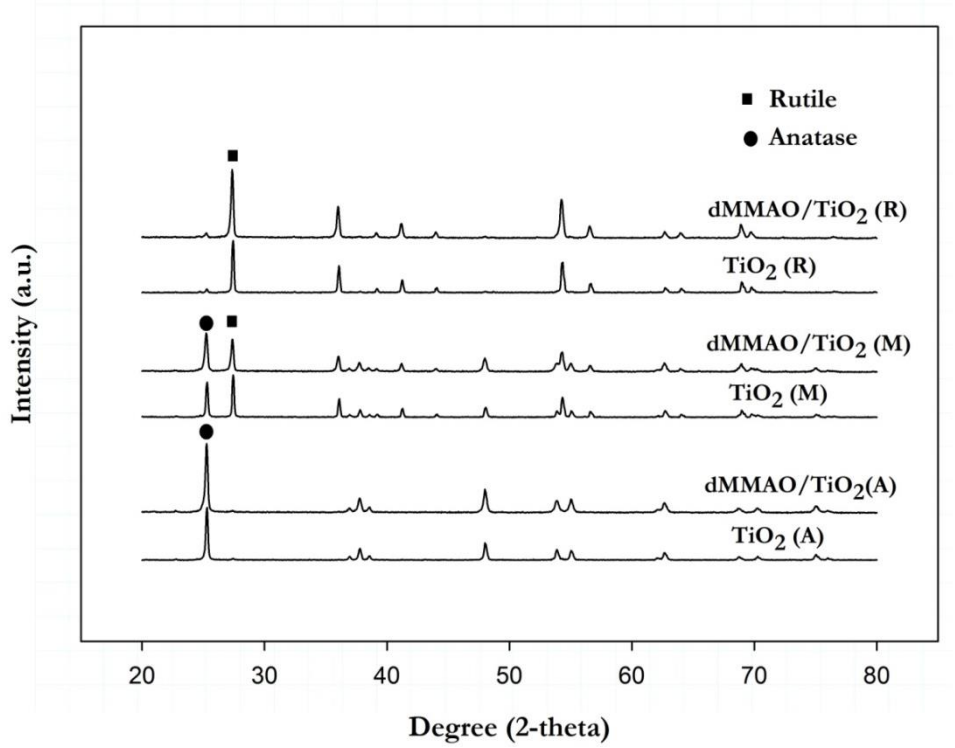

Fig. 1. XRD patterns of different TiO_2 supports before and after impregnation with dMMAO.

Figure 2 illustrates the transmission electron micrograph of different phases of titania before and after impregnation. The result shows that the anatase particles are almost in a spherical shape and have a uniform particle size of about 100 nm. The rectangular rutile titania has a particle size around 400 nm. Both anatase and rutile phase were presented in mixed phase, where the average particle size of mixed phase was around 100-200 nm. After impregnation, the particle size of dMMAO-supported titania became larger. In the case of dMMAO/TiO_2 (M), the average particle size was around 150-300 nm, which was about 1.5 times larger than that of the original titania. The larger particle was due to the adsorption of dMMAO onto titania support.

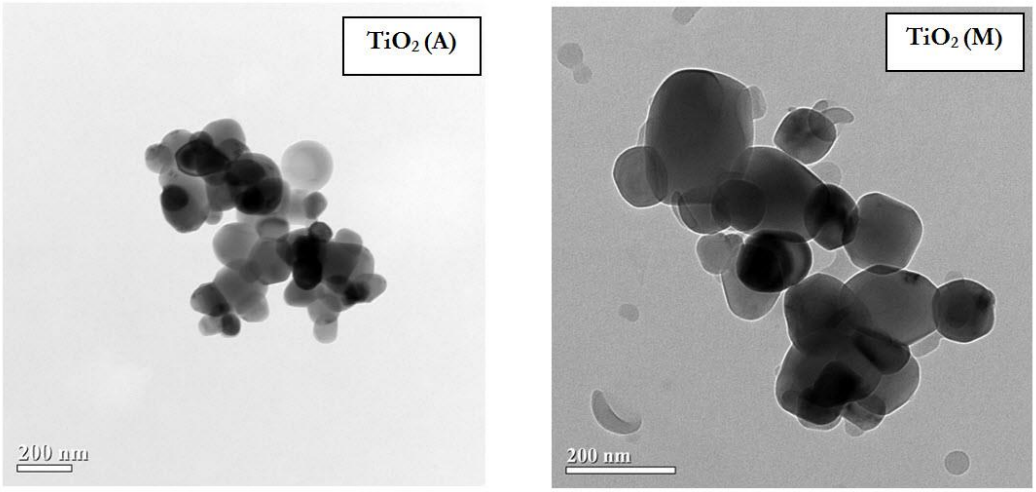

DOI:10.4186/ej.2015.19.5.55

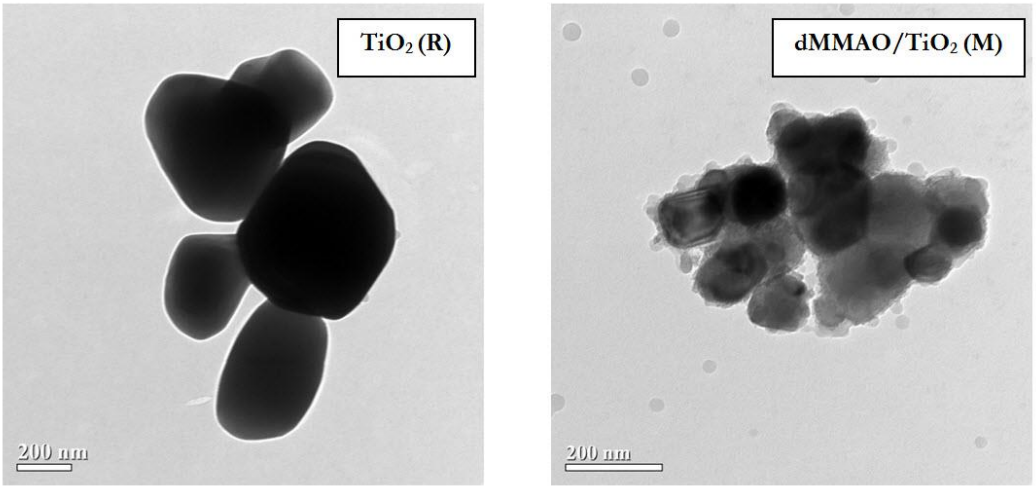

Fig. 2. TEM micrographs of different TiO_2 supports before and after impregnation with dMMAO.

To study the morphology and aluminium distribution over titania precursors, various samples were determined by SEM and EDX analyses. The SEM micrograph and EDX mapping for dMMAO/TiO_2 are shown in Fig. 3. It can be seen that Al of dMMAO was well distributed over precursor particle. The dMMAO absorption ability of different phases of titania are quite different, where the mixed phase seems to have low ability to absorb dMMAO. It is well known for metallocene catalyst that the amount of $[Al]_{dMMAO}$ plays an important role in the polymerization activity. This is because the metallocene catalyst would be activated with dMMAO to form metallocenium cations, which are regarded as the active species for polymerization. With an increase in the amount of $[Al]_{dMMAO,}$ the large amount of cationic species is generated and then the catalytic activity is increased. Thus, the dMMAO/TiO_2 precursors were analyzed to determine the $[Al]_{dMMAO}$ content by using EDX technique. The amount of $[Al]_{dMMAO}$ in various supports are reported in Table 2.

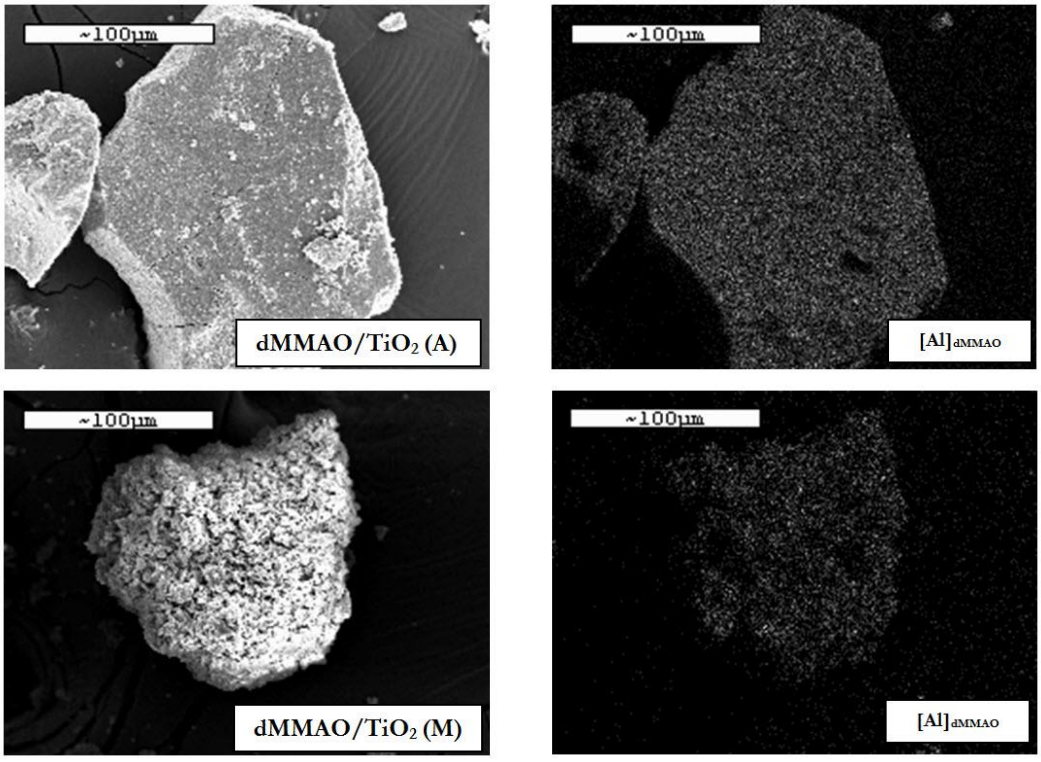

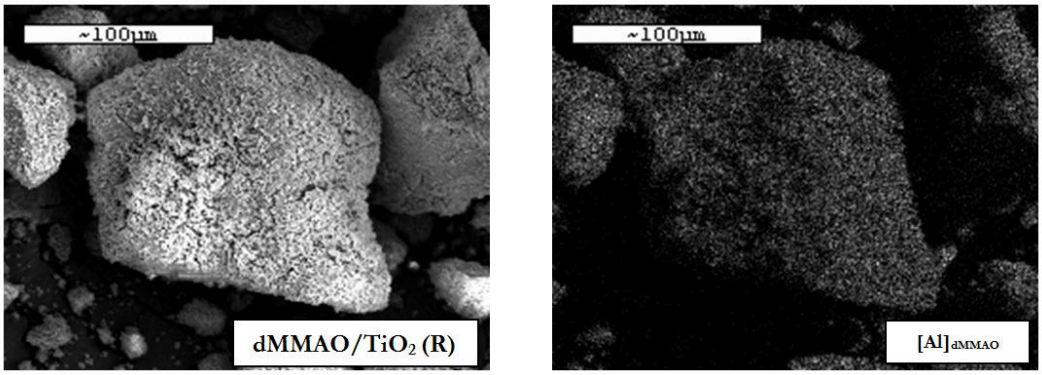

Fig. 3. SEM micrographs and EDX mapping for different dMMAO/TiO_2 supports.

According to those results, the amount of $[Al]_{dMMAO}$ on surface decreased in the order of dMMAO/TiO_2(A) > dMMAO/TiO_2(R) > dMMAO/TiO_2(M). The anatase phase possessed the highest amount of $[Al]_{dMMAO}$, probably due to its highest surface area. Most dMMAO are easily absorbed on the external surface, which is free from the internal diffusion resistance. Therefore, the $[Al]_{dMMAO}$ content on anatase was the highest. However, it should be noted that EDX is the surface chemical analysis. It only detects the dMMAO presented below the upper surface approximately 5 μm in depth. The result obtained from this analysis does not show the amount of $[Al]_{dMMAO}$ in bulk correctly. In order to confirm the amount of $[Al]_{dMMAO}$ presented in sample, ICP analysis is carried out. The result is shown in Table 2. Comparing the Al content measured by both techniques, the higher amount of $[Al]_{dMMAO}$ was found when determined by EDX. It suggests that dMMAO was mostly located on the external surface of titania rather than within the pore. Interestingly, although the amount of $[Al]_{dMMAO}$ on surface in anatase was higher than that in rutile and mixed phase, anatase had the lowest amount detected by ICP.

To evaluate the nature of the surface species, we conducted XPS analysis of dMMAO on various supports and investigated the binding energy (BE) of Al. The BE values for Al_{2p} of different precursors are listed in Table 2. It can be seen that the changes in BE are in the order of dMMAO/TiO_2(M) > dMMAO/TiO_2(R) > dMMAO/TiO_2(A). The result suggests that Al in dMMAO was affected by phase of titania employed. The anatase phase possessed the lowest BE. According to the literatures [7], the BE for Al_{2p} presented in dMMAO was around 74.9 eV. As we known, the BE refers to the energy levels of atomic core electrons. The high BE value for Al_{2p} suggested the strong interaction between Al in cocatalyst and titania support, owing to a low electron density of Al in cocatalyst. Thus, the strong Lewis acidity of dMMAO resulted in high BE value for Al_{2p}. The active species of metallocene catalyst is an ion-pair of a metallocenium cation and anion derived from cocatalyst. An increase in the Lewis acidity of cocatalyst leads to more strongly abstraction of methyl group from metallocene. The formation of coordinatively unsaturated–active species is enhanced, and then the catalytic activity is increased. However, much more Lewis acidity of cocatalyst can lead to the formation of contact ion-pair, thus the catalytic activity would be decreased. To clarify the catalytic behavior, the polymerization was tested and the results are shown below.

Table 2. Al contents obtained from EDX and ICP, and XPS binding energy of various supports.

Type of catalyst precursor	$[Al]_{dMMAO}$ in catalyst precursor (%wt)		BE (eV)[a] for Al_{2p}
	EDX	ICP	
dMMAO/TiO_2(A)	22.8	16.8	74.5
dMMAO/TiO_2(M)	19.1	18.0	75.1
dMMAO/TiO_2(R)	22.0	19.1	75.0

[a] Obtained from XPS.

3.2. Catalytic activity

Copolymerization of ethylene and 1-hexene over titania supported zirconocene/dMMAO catalysts was investigated. The catalytic activities are summarized in Table 3. The results show that the copolymerization activities for all catalysts were in the order of homogeneous system > TiO_2 (A) > TiO_2 (R) > TiO_2 (M).

The homogeneous catalyst exhibited higher catalytic activity than the heterogeneous one. The reduction in activity was attributed to the impurities presented on support surface and/or the steric hindrance caused by support which hinder the access of monomer to active sites [23, 24]. Among the supported catalysts, TiO_2 (A) exhibited the highest catalytic activity, while TiO_2 (M) showed the lowest. The better activity in anatase can be attributed to the higher active site at its external surface. Although the amount of $[Al]_{dMMAO}$ plays an important role in the catalytic activity, based on our experiment the ratio of $[Al]_{dMMAO}/[Zr]_{cat}$ was fixed at 1135 for all runs. Hence, another factor influencing the catalytic activity may be the interaction of $[Al]_{dMMAO}$ and titania support as well as the dispersion of dMMAO over precursor.

Table 3. Polymerization activities for different TiO_2 supports[a].

Sample	Reaction time (s)	Polymer yield (g)	Catalytic activity (kg polymer/mol Zr·h)
Homogeneous	126	1.36	25,905
TiO_2 (A)	138	0.98	17,107
TiO_2 (M)	193	0.77	9,594
TiO_2 (R)	144	0.79	13,162

[a]Polymerization conditions: $[Al]_{dMMAO}/[Zr]_{cat}$ = 1135 (calculated from ICP/AES), $[Al]_{TMA}/[Zr]_{cat}$ = 2500, $[Zr]_{cat} = 5\times10^{-5}$ M, solvent = toluene, total volume =30 mL, temperature = 343 K.

In order to prove the interaction of $[Al]_{dMMAO}$ and support, TGA measurement was performed. In the case of dMMAO-supported system, the hydroxyl groups on support react with dMMAO, forming a covalent bond through the $O_{support}–Al_{cocatalyst}$ linkage. Result of TGA reports the degree of interaction for dMMAO and support in terms of weight loss and decomposition temperature. The weaker interaction leads to some leaching of cocatalyst from support, resulting in low active species. On the contrary, too strong interaction between cocatalyst and support can cause more difficultly for zirconocene catalyst to react with dMMAO during activation step, resulted in the lower catalytic activity. Thus, the optimum degree of interaction is required to achieve high catalytic activity. The TGA profiles for different dMMAO/TiO_2 are shown in Fig. 4. The weight loss of catalyst precursor was in the order of TiO_2 (R) (21.42%) > TiO_2 (M) (17.32%) > TiO_2 (A) (16.15%). It also corresponds with the thermal decomposition temperature at 10% weight loss ($T_{d10\%}$), which increased as follows: TiO_2 (R) (224°C) > TiO_2 (M) (272°C) > TiO_2 (A) (275°C). It can be concluded that the highest catalytic activity for TiO_2 (A) was due to the strongest interaction. These results are in agreement with Chaichana et al. [25], which reported that the strong interaction between cocatalyst and support is considerable; otherwise some leaching would occur during washing and drying steps in ex situ impregnation method. In comparison to mixed phase, rutile phase exhibited higher catalytic activity although it possessed the lower degree of interaction. The reason might be due to the better dispersion of its $[Al]_{dMMAO}$ over titania as measured by EDX mapping.

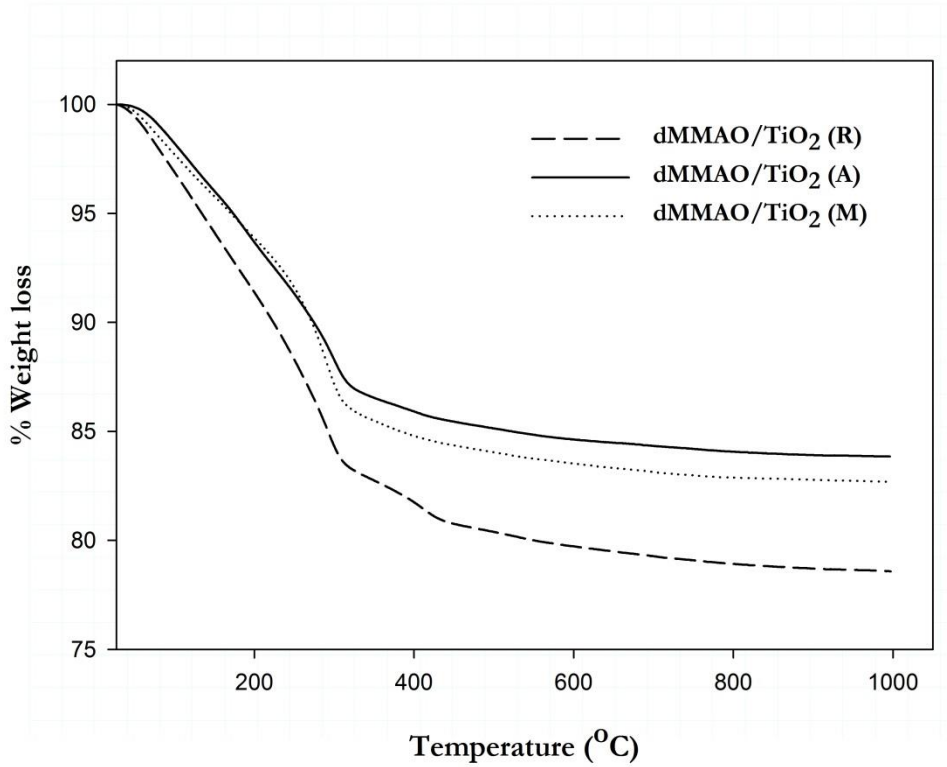

Fig. 4. TGA profiles of $[Al]_{dMMAO}$ on different TiO_2 supports.

In addition, according to the XPS results, it was found that the catalytic activity was correlated to the BE value for Al_{2p} in the supported systems. The relationship between BE and catalytic activity for various dMMAO/TiO_2 is presented in Fig. 5, which shows that the activity decreased with an increase in BE value. The higher catalytic activity can be explained by a weaker coordination of cationic species and cocatalyst-derived anion, which caused by a lower Lewis acidity of dMMAO/TiO_2. The separation of ion-pair was enhanced, and the propagation rate was increased. On the contrary, the higher Lewis acidity makes the coordinated metallocenium cation and dMMAO anion to be stronger, leading to the formation of contact ion-pair. Hence, the catalytic activity was decreased.

DOI:10.4186/ej.2015.19.5.55

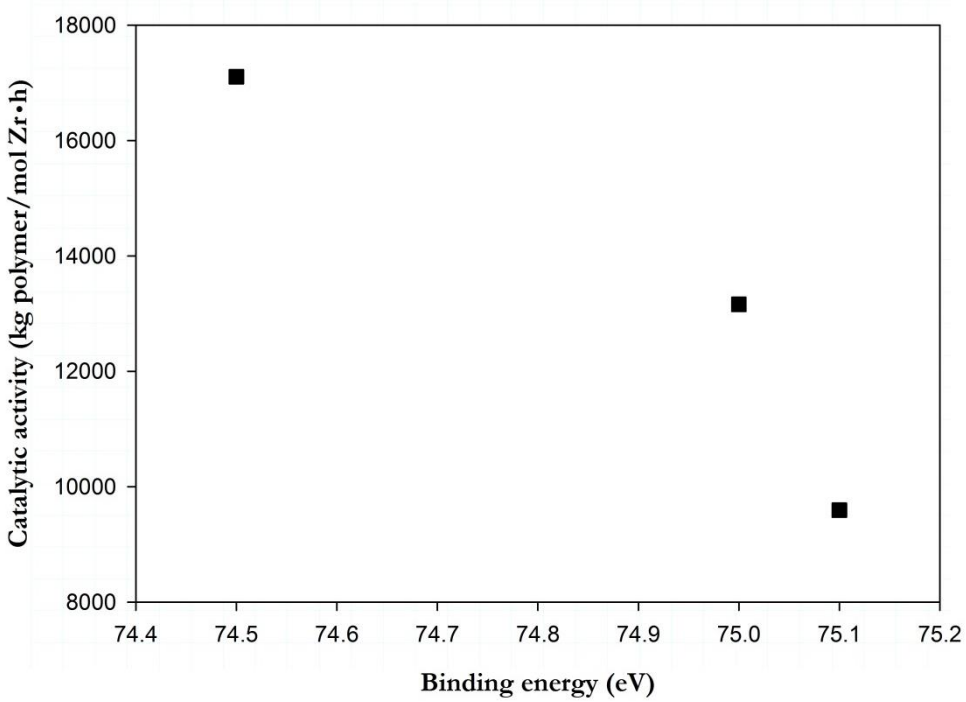

Fig. 5. Relationship between binding energy (BE) of Al_{2p} of dMMAO on the supports and the catalytic activity.

3.3. Polymer Characteristic

To determine the polymer properties, the obtained LLDPEs were characterized by SEM/EDX, ^{13}C NMR and DSC analyses. SEM images in Fig. 5 shows that the LLDPE copolymers covered on the titania support and the reactor fouling did not found after polymerization. There was no significant difference in the polymer morphology upon the different phases of titania were employed. The produced LLDPEs are mostly spherical in shape for all titania-based catalysts. The sample particles were around 100 to 150 μm in size, which was about 1000 times larger than that of the original titania particles. The LLDPE produced from rutile phase was larger size than that from anatase and mixed phase. Also, the good distribution of titania inside the polymer particle can be seen as shown in Fig. 6.

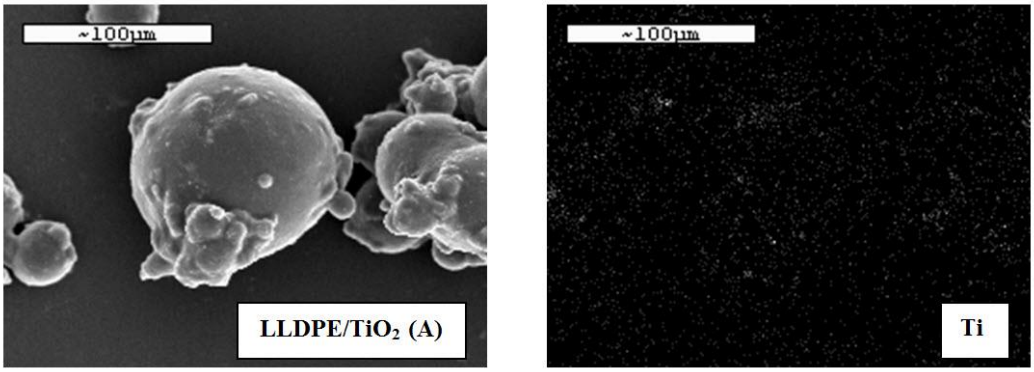

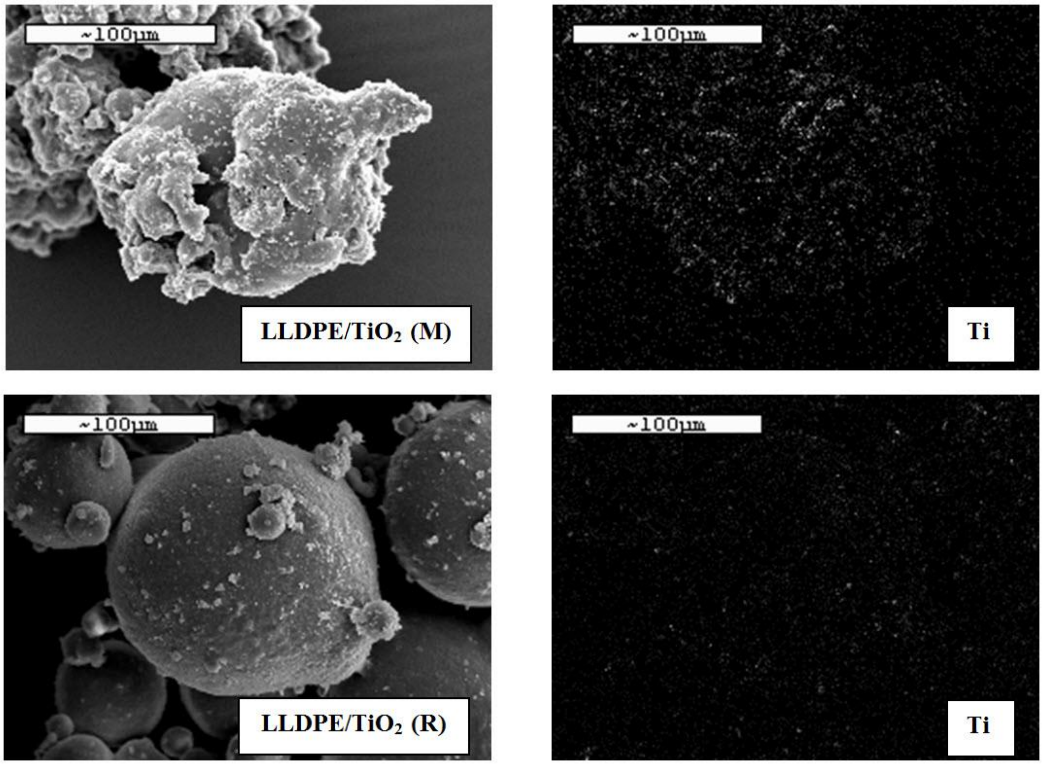

Fig. 6. SEM micrographs of LLDPE/TiO_2 and Ti distribution obtained from EDX upon different TiO_2 supports.

The obtained polymers were further characterized by ^{13}C NMR spectroscopy. The triad distributions of the comonomer were calculated according to literature [22]. The results are presented in Table 5, which shows that the distributions in copolymer are almost the same. The EEE triad was predominant, while the HHH triad was negligible. The 1-hexene incorporations in copolymers were determined from the triad contents and shown in Table 5. It was found that LLDPE from anatase possessed the highest ability for 1-hexene incorporation. Due to its high amount of $[Al]_{dMMAO}$ over surface as determined by EDX, the most active sites for copolymerization were located on the external surface, which is easily for 1-hexene to reach active site and incorporate into polymer chain. Thus, the lower steric hindrance over surface led to an increase in the 1-hexene incorporation ability (scheme 1). DSC measurement indicated that all systems produced polymers with melting temperatures around 82-90°C. The measured melting temperature was lower than that the conventional LLDPE (~120°C). The lower melting temperature is due to the higher insertion of 1-hexene (>10 mol%). The melting temperature of the LLDPE is dependent on the content of 1-hexene incorporation. So, the polymer produced from anatase phase had the lowest melting temperature.

Table 5. Triad distribution of LLDPE/TiO_2 copolymer obtained from ^{13}C NMR analysis and thermal property from DSC measurement.

System	Triad distribution of copolymer[a]						1-hexene insertion[b] (mol %)	T_m[c] (°C)
	EEE	EEH	HEH	EHE	EHH	HHH		
TiO_2 (A)	0.245	0.283	0.094	0.095	0.283	0.000	38	82
TiO_2 (M)	0.554	0.180	0.050	0.065	0.151	0.000	22	90
TiO_2 (R)	0.358	0.300	0.055	0.123	0.164	0.000	29	83

[a]E refers to ethylene monomer and H refers to 1-hexene comonomer.
[b]Content of 1-hexene in the copolymer from ^{13}C NMR.
[c]Obtained from DSC.

DOI:10.4186/ej.2015.19.5.55

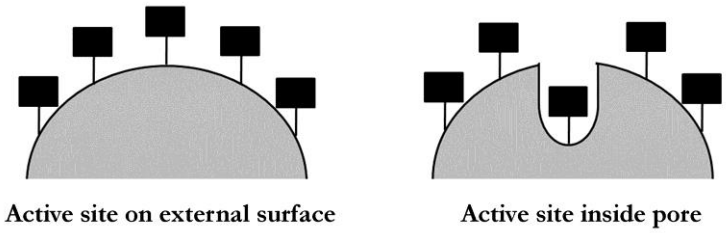

Scheme. 1. Location of active sites over different TiO_2 supports.

4. Conclusion

Copolymerization of ethylene and 1-hexene over titania supported zirconocene/dMMAO catalyst was performed. The different phases of titania affected both catalytic activity and properties of polymer. Based on EDX results, after impregnation with dMMAO, the cocatalyst almost located on the external surface of titania. The highest catalytic activity of TiO_2 (A) is attributed to the stronger interaction between cocatalyst and support as determined by TGA. The good dispersion of dMMAO also plays an important role in the catalytic performance. LLDPE produced with TiO_2 (A) exhibited higher 1-hexene incorporation and lower melting point in comparison with that produced with other titanias.

Acknowledgement

The authors thank the Thailand Research Fund (TRF), National Research University Project, Office of the Higher Education Commission (WCU029-AM57) for the financial support of this project. We also would like to thank Post Doctoral Scholarship for supporting this research.

References

[1] R. Van Grieken, A. Carrero, I. Suarez, and B. Paredes, "Effect of 1-hexene comonomer on polyethylene particle growth and kinetic profiles," *Macromolecular Symposium*, vol. 259, no. 1, pp. 243–252, 2007.

[2] C. Piel, P. Starck, J. V. Seppälä, and W. Kaminsky, "Thermal and mechanical analysis of metallocene-catalyzed ethene–α-olefin copolymers: The influence of the length and number of the crystallizing side chains," *Journal of Polymer Science Part A: Polymer Chemistry*, vol. 44, no. 5, pp. 1600–1612, 2006.

[3] H. W. Park, J. S. Chung, S. S. Lim, and I. K. Song, "Chemical composition distributions and microstructures of ethylene–hexene copolymers produced by a *rac*-Et(Ind)$_2$ZrCl$_2$/TiCl$_4$/MAO/SMB catalyst," *Journal of Molecular Catalysis A: Chemical*, vol. 264, no. 1, pp. 202–207, 2007.

[4] W. Kaminsky, "The discovery of metallocene catalysts and their present state of the art," *Journal of Polymer Science Part A: Polymer Chemistry*, vol. 42, no. 16, pp. 3911–3921, 2004.

[5] J. A. Ewen, "Symmetry rules and reaction mechanisms of Ziegler–Natta catalysts," *Journal of Molecular Catalysis A: Chemical*, vol. 128, no. 1, pp. 103–109, 1998.

[6] B. Paredes, J. B. Soares, R. van Grieken, A. Carrero, and I. Suarez, "Characterization of ethylene-1-hexene copolymers made with supported metallocene catalysts: Influence of support type," *Macromolecular Symposium*, vol. 257, no. 1, pp. 103–111, 2007.

[7] H. Hagimoto, T. Shiono, and T. Ikeda, "Supporting effects of methylaluminoxane on the living polymerization of propylene with a chelating (diamide)dimethyltitanium complex," *Macromolecular Chemistry and Physics*, vol. 205, no. 1, pp. 19–26, 2004.

[8] K. T. Li, C. L. Dai, and C. Y. Li, "Synthesis of linear low density polyethylene with a nano-sized silica supported Cp$_2$ZrCl$_2$/MAO catalyst," *Polymer Bulletin*, vol. 64, no. 8, pp. 749–759, 2010.

[9] S. Jüngling, S. Koltzenburg, and R. Mülhaupt, "Propene homo- and copolymerization using homogeneous and supported metallocene catalysts based on Me$_2$Si(2-Me-Benz[e]Ind)$_2$ZrCl$_2$," *Journal of Polymer Science Part A: Polymer Chemistry*, vol. 35, no. 1, pp. 1–8, 1997.

[10] B. Jongsomjit, P. Kaewkrajang, and P. Praserthdam. "Effect of silane-modified silica/MAO-supported Et[Ind]$_2$ZrCl$_2$ metallocene catalyst on copolymerization of ethylene," *European Polymer Journal*, vol. 40, no. 12, pp. 2813–2817, 2004.
[11] Ł. Korach, and K. Czaja, "Synthesis and activity of zirconocene catalysts supported on silica-type sol-gel carrier for ethylene polymerization," *Polymer Bulletin*, vol. 46, pp. 175–182, 2001.
[12] M. de Fátima V Marques, and M. de Alcantara, "Alumina as support for metallocene catalyst in ethylene polymerization," *Journal of Polymer Science Part A: Polymer Chemistry*, vol. 42, no. 1, pp. 9–21, 2004.
[13] K. Saga, and M. Kaminaka, "Copolymerization of olefins with SiO_2-, Al_2O_3-, and $MgCl_2$-supported metallocene catalysts activated by trialkylaluminiums," *Macromolecular Chemistry and Physics*, vol. 195, no. 4, pp. 1369–1379, 1994.
[14] W. Owpradit, and B. Jongsomjit, "A comparative study on synthesis of LLDPE/TiO_2 nanocomposites using different TiO_2 by *in situ* polymerization with zirconocene/dMMAO catalyst," *Macromolecular Chemistry and Physics*, vol. 112, no. 3, pp. 954–961, 2008.
[15] E. Chaichana, S. Pathomsap, T. Shiono, and B. Jongsomjit "Observation of bimodal LLDPE/TiO_2 nanocomposites produced by *in situ* polymerization with zirconocene/MMAO catalysts via Ga modification on TiO_2 nanofiller," *Engineering Journal*, vol. 17, no. 3, pp. 33–42, 2013.
[16] S. Amornlertpreecha, T. Shiono, and B. Jongsomjit, "Copolymerization of ethylene/1-olefin with mesoporous titania-supported zirconocene/MAO catalyst," *Engineering Journal*, vol. 16, no. 5, pp. 9–15, 2012.
[17] C. Ketloy, B. Jongsomjit, and P. Praserthdam "Characteristics and catalytic properties of [*t*-BuNSiMe$_2$Flu]TiMe$_2$/dMMAO catalyst dispersed on various supports towards ethylene/1-octene copolymerization," *Applied Catalysis A*, vol. 327, no. 2, pp. 270–277, 2007.
[18] E. Chaichana, S. Pathomsap, O. Mekasuwandumrong, J. Panpranot, A. Shotipruk, and B. Jongsomjit, "LLDPE/TiO_2 nanocomposites produced from different crystallite sizes of TiO_2 via *in situ* polymerization," *Chinese Science Bulletin*, vol. 57, no. 17, pp. 2177–2184, 2012.
[19] A. M. Domínguez, A. Zárate, R. Quijada, and T. López, "Sol–gel iron complex catalysts supported on TiO_2 for ethylene polymerization," *Journal of Molecular Catalysis A: Chemical*, vol. 207, no. 2, pp. 155–161, 2004.
[20] T. Hasan, A. Ioku, K. Nishii, T. Shiono, and T. Ikeda, "Syndiospecific living polymerization of propene with [*t*-BuNSiMe$_2$Flu]TiMe$_2$ using MAO as cocatalyst," *Macromolecules*, vol. 34, no. 10, pp. 3142–3145, 2001.
[21] H. Hagimoto, T. Shiono, and T. Ikeda, "Living polymerization of propene with a chelating diamide complex of titanium using dried methylaluminoxane," *Macromolecular Rapid Communications*, vol. 23, no. 1, pp. 73–76, 2002.
[22] K. Soga, T. Uozumi, and J. R. Park, "Effect of catalyst isospecificity on olefin copolymerization," *Die Makromolekulare Chemie*, vol. 191, no. 12, pp. 2853–2864, 1990.
[23] F. AlObaidi, Z. Ye, and S. Zhu, "Ethylene polymerization with silica-supported nickel-diimine catalyst: Effect of support and polymerization conditions on catalyst activity and polymer properties," *Macromolecular Chemistry and Physics*, vol. 204, no. 13, pp. 1653–1659, 2003.
[24] Y. Choi, and J. B. Soares, "Synthesis of supported nickel diimine catalysts for ethylene slurry polymerization," *Macromolecular Chemistry and Physics*, vol. 210, no. 22, pp. 1979–1988, 2009.
[25] E. Chaichana, T. Shiono, P. Praserthdam, and B. Jongsomjit, "A comparative study of *in situ* and *ex situ* impregnation for LLDPE/silica composites production," *Engineering Journal*, vol. 16, no. 1, pp. 27––36, 2011.